Downscaling long term socio-economic scenarios at city scale: a case study on Paris

Vincent Viguié[a,1,*], Stéphane Hallegatte[b,c,2], Julie Rozenberg[a]

[a]*Centre International de Recherche sur l'Environnment et le Développement, Paris, France*
[b]*The World Bank, Washington D.C.*
[c]*Ecole Nationale de la Météorologie, Météo-France, Toulouse, France*

Abstract

The NEDUM-2D model is used to downscale four global socio-economic scenarios at city scale and simulate the evolution of the Paris urban area between 1900 and 2100. It is based on a dynamic extension of the classical urban economic theory, to explain the spatial distribution of land and real estate values, dwelling surfaces, population density and buildings heights and density. A validation over the 1900-2010 period shows that the model reproduces available data and captures the main determinants of city shape evolution. From four global scenarios and additional local inputs, 32 local scenarios are created and analyzed. Main drivers of urban sprawl and climate and flood vulnerability appear to be local demographic growth and local policies; global factors, such as energy and transport prices, even including possible peak-oil and carbon taxes, have only a limited influence on them. Conversely, transport-related greenhouse gases emissions are mainly driven by global factors, namely vehicle efficiency changes, not by land use. As a consequence, very strict urban policies — including reconstruction — would become necessary to control emissions from urban transportation if technologies reveal unable to do so. These scenarios are a useful input for the design and assessment of mitigation and adaptation policies at local scale.

Keywords: urban planning, urban sprawl, carbon tax, mitigation, adaptation, scenarios

*Corresponding author

Email address: viguie@centre-cired.fr (Vincent Viguié)

[1]Tel: (33) 1 43 94 73 03 Fax: (33) 1 43 94 73 70, CIRED, Site du Jardin Tropical, 45bis, Av de la Belle Gabrielle F-94736 Nogent-sur-Marne, France

[2]The findings, interpretations, and conclusions expressed in this paper are entirely those of the authors. They do not necessarily represent the views of the International Bank for reconstruction and Development/World Bank and its affiliated organizations, or those of the Executive Directors of the World Bank or the governments they represent.

1. Introduction

Climate change adds new and unprecedented challenges to urban planning. Urban transport, land-use, and housing policies are indeed increasingly recognized as major tools for climate change mitigation (e.g., [1, 2, 3]). At the same time, due to their high concentration in population and economic activity, cities are particularly vulnerable to climate change impacts, and their vulnerability is greatly determined by city structure. Urban adaptation policies will thus need to be developed ([4, 5, 6]).

Downscaling long term global socio-economic scenarios at city scale is useful at the urban area level, to help local decision-making develop these local adaptation and mitigation policies. Indeed, using urban planning as a tool for mitigation and adaptation is made extremely difficult by the high inertia of city built structure ([7, 8]). Anticipated action is required if one wants cities to be adapted to the climate of the end of the century and to contribute less to global CO_2 emissions. But the impacts of policies depend on several external factors: demographic, socio-economic, cultural, political and technological changes will play a major role. For instance, success of strategies aiming at reducing transport energy consumption is dependent on future transport prices. Prospective studies that explore various possible evolutions of these variables are thus required to design the best policies.

This exercise is also useful on a global scale, as scenarios on the evolution of urban forms would also be relevant for the building of long-term narratives of future greenhouse gases emissions ([9, 10, 11, 12]), and future climate change vulnerability ([13, 14]).

A growing body of literature is now trying to establish such long term scenarios (often until 2100) at city scale and related to global environmental change for climate change impacts or mitigation analysis ([15, 9, 16, 17, 18, 19]). Such long-term scenarios related to global environmental change are different from traditional city scenarios designed to support urban planning, which generally consider time horizons of 30 years or less and are not connected to global scenarios, in which global environmental change can be represented (cf. for instance [20, 21], or studies listed in [22]).

In our study, the NEDUM-2D model[3] is used to simulate the evolution of the Paris urban area between 1900 and 2100. It uses a dynamic extension of the classical urban economic theory to explain the spatial distribution of land and real estate values, dwelling surfaces, population density and buildings heights and density. A validation over the 1900-2010 period shows that the model reproduces fairly faithfully the available data and captures the main determinants of city shape evolution, suggesting that this tool can be used to inform policy decisions. Our approach is, a priori, applicable to most urban areas where data is available.

In Section 2, we briefly present our model and its equations. Section 3 presents the results of the model calibration and its validation over past evolution of Paris urban area. Section 4 describes the hypotheses that have been used in our scenarios. Section 5 investigates the results of our simulations, and draw general conclusions regarding climate change mitigation

[3] Source code available upon request.

and adaptation. Finally, Section 6 concludes.

2. Modelling urban growth

Although models are highly simplified descriptions of reality, they are useful to create prospective scenarios. By enabling decision makers and stakeholders to understand the main mechanisms and interactions between variables, they can create a basis for policy discussion. It should be highlighted that prospective scenarios do not "predict" the future. They are possible and coherent scenarios, which represent conceivable futures in the spirit of the SRES scenarios ([23, 24]). Prospective scenarios can fuel the debates about Paris future and inform policy-making, but they have no predictive value.

Several methods can be used to create scenarios for urban development and extensive reviews of land-use change models exist (for examples, see [22, 25]). One first set of methods extrapolates past tendencies: it studies past evolution of the city to anticipate its future. Models can rely on statistical regressions (see for instance [26]), Markov chains or cellular automata (see for instance [9]). A second set of methods proposes to model main evolution drivers, especially land-use transport interaction (see [27], for a review). The main disadvantage of this method is that many phenomena are neglected : the outcome is only an approximation of reality. The main advantage is that the simulations are easily understandable, as is the influence of each parameter, and that these models are based on mechanisms that are supposed to remain valid in the future, while past-trends extrapolation is always questionable.

This analysis is based on such a model of city evolution. To produce scenarios going until the end of the century, it uses only general and fundamental economic principles, which are likely to remain constant over the long term.

The model we use here, NEDUM-2D, is able to capture the dynamics of urban systems, and the importance of inertia. It is based on a model developed in Gusdorf and Hallegatte [7, 28], Gusdorf et al. [8], Viguié and Hallegatte [29, 30], Viguié [31]. It is a dynamic model which relies on the classical urban economics framework, an economic modeling approach developed since the end of the 1960s ([32, 33, 34]) which explains the spatial distribution — across the city — of the costs of land and of real estate, housing surface, population density and buildings heights and density.

As explained in Gusdorf et al. [8], urban economics has been mostly used to explore the characteristics of long run equilibriums. However, the existence of urban stationary equilibriums is questionable: when population, transport prices, or income vary, housing infrastructure cannot adapt rapidly to changing conditions and is always out of equilibrium. Our model takes explicitly into account this dynamics and describes cities as non-equilibrium systems.

A complete description of the model, with the full set of equations, is available in Appendix A. It is based on three main mechanisms.

First, we suppose that households choose their accommodation location and size by making a trade-off between the time and money they spend in transport (i.e. to commute to their jobs)

and the real estate price level (or, equivalently, between the proximity to the city center and the housing surface they can afford).

Second, real estate developers choose to build more or less housing (i.e. larger or smaller building) at a specific location, depending on the local level of real estate prices. When these prices are low, developers tend to build low density buildings, and when these prices are high, they tend to build high density buildings.

Third, we suppose that various city characteristics do not evolve and adjust at the same speed. For instance, rents can evolve very quickly, whereas buildings change with a much longer timescale. Building depreciation is also very low, leading to path dependency and lock-ins in city evolution.

Using these mechanisms, it is possible to determine the structure of the city from information on population size, households' income, transport network location, building construction costs and developers behavior parameters.

Let us present briefly two classical results of urban economics which are of relevance for our analysis.[4] These results are still valid in our modeling. The first is that variation of real estate prices across the urban area is uniquely determined by transport generalized prices. An increase in transport price (or a decrease in transport speed) results in a steeper decrease in real estate prices with distance from the center. Developers react to this change, and population density tends to increase, or decrease, where real estate prices respectively increase or decrease. Conversely, a decrease of transport prices makes real estate prices decrease less steeply with distance, i.e. real estate prices become more homogeneous in the city. Developers also react to this change, and population density becomes more homogeneous, too.

Secondly, if transport generalized price enables to compute variation of real estate prices across the urban area, the overall level of real estate prices is mostly determined by available ground space and by the number of inhabitants. Let us suppose for instance that available ground space decreases, or that the city population increases. In this case, according to urban economic theory, real estate prices will increase everywhere. Because of this increase, developers will build more, and population density will increase everywhere (until all the population can be accommodated). It should be highlighted that, in this case, if transport generalized prices do not change, the relative distribution of real estate prices across the urban area does not change. In this case, all real estate prices increase or decrease by the same amount, everywhere in the urban area.

A combination of transport prices decrease and available ground space decrease leads both to an increase of average real estate prices level, and to more homogeneous real estate prices. Real estate price variation in the center of the city can therefore be either positive or negative, according to the relative magnitude of the transport price decrease and the ground space decrease.

[4]For a detailed analysis of urban economic framework see Fujita [35].

3. Calibration and Validation

3.1. Model hypotheses

This section summarizes the model calibration.

First, we suppose that there exists a unique city center. If, rigorously speaking, recent trends in Paris urban area development seem to contradict this assumption, it is still reasonable to accept it, at least in first approximation, as can be seen in Section 3.4 : rents and population density reach a peak at a point that corresponds to the center of Paris and decrease in all directions on a regular basis when one moves away. High job density near the center of Paris[5] and Paris urban area star-shaped public transport network, which means that a large fraction of people working outside the center have to go through the center to commute, also contribute to the relevance of the monocentric approach. Results presented below confirm that the monocentric assumption is still able to explain the major characteristics of the Paris urban area up to now.

For a question of simplicity and clarity, we have developed scenarios in which the urban area keeps evolving in a monocentric way. This prevents from analyzing some possible future developments, especially if Paris urban area becomes more polycentric than it actually is.[6] As for all following hypotheses, this should be considered as a selection of a set of scenarios among many possible others. Based on the numerous theoretical frameworks which have been proposed to account for decentralized production and to incorporate amenities (see for instance [36, 37, 38, 39, 40, 41, 42, 43]), we introduce in an on-going study a tendency towards polycentrism in the model, by modelling firms (and employment) location choices. However these theoretical extensions are not included in the present analysis.

Second, this model only is based on market mechanisms. In practice, because of urbanism constraints (e.g. limits to building heights) and of direct public investment (e.g. in public housing or infrastructure), the structure of the Paris urban area does not directly correspond to the resulting balance of the free play of market. We introduce explicitly constraints of this type in the model: we limite the height of buildings in Paris and forbid to build in some areas (natural parks, public gardens...). We do not describe direct public investment aiming at changing the urban shape. For instance, "Villes nouvelles" ("new towns")[7] are an historic example of a planned urban development that the model is not able to anticipate. Thus, the model provides spontaneous urbanization trends, that urban policy may alter.

[5] For instance, 60% of all jobs of Paris urban area administrative region (Île de France) lie within 12km from the center of Paris, i.e. in a circle with an area representing less than 4% of Île de France area. (Source: INSEE)

[6] Many possible changes could actually favor such an evolution : (1) major development of telecommuting would change the housing patterns (people may decide to live much further if they do not have to commute everyday); (2) change in infrastructure patterns with a new network that is not star-shaped (this is unlikely considering the legacy of current infrastructure and planned investments); (3) changes in transport technologies, such as the driverless car (which could lead to less or more sprawl depending on how it is used); (4) population aging that may increase the fraction of the population that does not work and does not have to commute everyday.

[7] These new towns were created from scratch in France in the mid-1960s to try to control the expansion of several cities. For example Cergy-Pontoise, Marne-la-Vallée, Sénart, Évry and Saint-Quentin-en-Yvelines were created around Paris.

We also exclude social housing from our study, because it is strongly regulated and do not follow market forces. Since the access to social housing is constrained in practice[8], we assume that the existence of social housing has a limited influence on the private market. More precisely, we assume that households cannot make social housing and private housing compete, which would result in a reduction of private real estate prices until they become comparable to social housing prices.

Given the level of abstraction and the exploratory nature of this work, we have here neglected the local distribution of household income. One obvious development of this study is the introduction of the households heterogeneity (including income differences) in the analysis.

3.2. Data and coefficients

All data and coefficients used in the simulations are summed up in Appendix B. To compute generalized transport prices, we used data about walking times, actual transport times and prices in public transport (underground, regional trains and suburban trains) and private transport (during rush hours, for an average car). At each location, the generalized transport cost is computed for each transport mode, and a logit weighting is used to compute the modal shares.[9] In the simulations, changes in public and private transport prices lead therefore to modal shifts.

We suppose in the simulations that construction costs and value of time evolve, over time, proportionally to households average income. This a strong hypothesis, with important implications on model results (cf. Section 5.1).

Concerning the cost of time, our hypothesis is coherent with the relevant literature (see for instance [45]). However, it should be noted that technological innovations that make travel more comfortable reduce the cost of time (i.e. the monetary equivalent of spending one minute in traveling, expressed as a fraction of the hourly net wage). Therefore, a constant trend towards more comfortable means of transport would result in a cost of time increasing less than proportionally to income. Empirical studies have captured this phenomenon ([46]). Here, we neglect this phenomenon (cf. Section 5.1 for a discussion of the consequences).

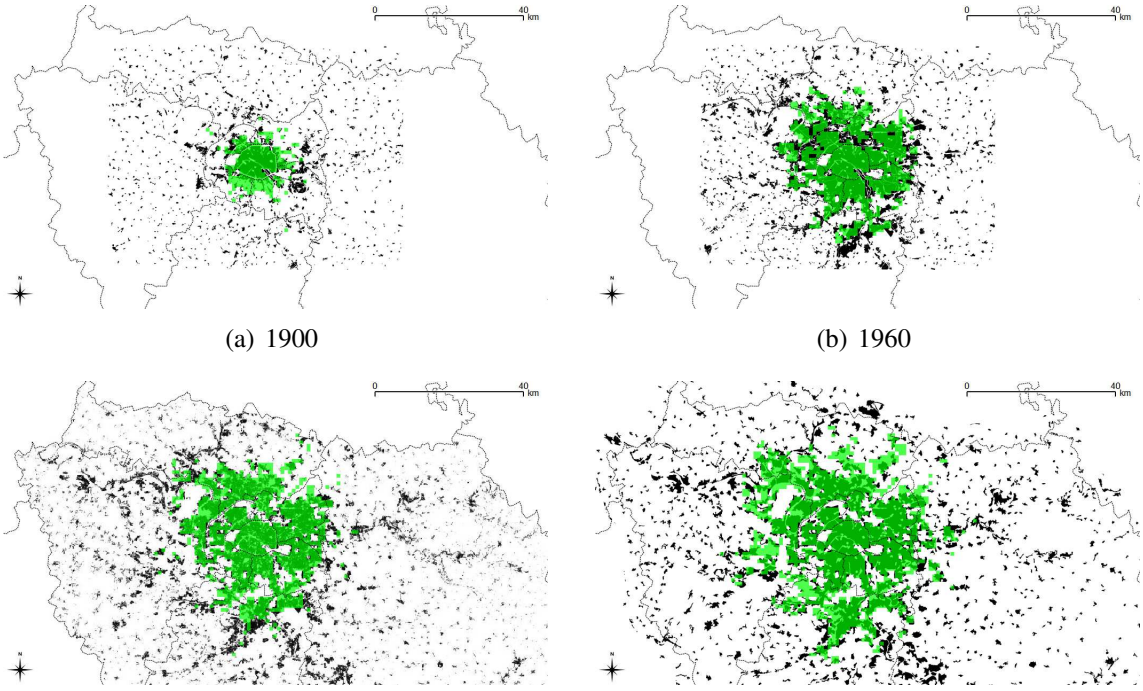
It proves difficult to find analyses of long term evolution of construction costs over time. To the authors' knowledge, no data exist in the relevant literature. If construction price indexes are measured in many countries, they are generally measured for constant-quality dwelling, and do not take into account the evolution of preferences and construction norms. It is therefore difficult to assess how construction costs have evolved in the past. We suppose that these costs evolve proportionally to households income.

3.3. Urban area evolution

As can be seen on Fig. 1(d), the model reproduces well the current Paris urban area. The main mismatch is in the west (Mantes la Jolie) and in the south of the urban area (Melun), where

[8] In 2007, for instance, only about 7% of demand for social housing in Île de France was fulfilled ([44]).

[9] More rigorously, at each location, the logit weighting is computed on each price divided by the minimum price at this location.



(a) 1900 (b) 1960

(c) 1982 (d) 2008

Figure 1: Simulated urbanized area compared to actual urbanized area. Actual urban area appears in black (Source: IAU, MOS database), whereas model simulation appears in transparent green.

the model does not capture observed urbanized areas. These two zones correspond to cities which were built long before being included in Paris urban area, and are important employment centers on their own, whereas the model only represents built areas due to Paris urban area sprawl.

It is possible to use this model to simulate city evolution from 1900 to 2008. For instance, Fig. 1(a), Fig. 1(b) and Fig. 1(c) compare simulated urban area with actual urbanized area, in 1900, 1960 and 1982, respectively. Because of the lack of data, we used the same transport network as in 2008 to do these three simulations, and the description of the city in 1900 is not as good as for the following years[10]. However, large-scale trends between 1900 and 2008 are well described, suggesting that the model captures the main determinants of city shape evolution.

3.4. Internal city structure

As shown in Fig. 2(a) the model describes the distribution of rents across the city in 2008 satisfactorily. In two dimensions, the model explains 51.8% of the variance in rents. When all areas at a given distance from the center are averaged, the model explains 89.5% of the uni-dimensional variance. Figure 2(b) shows that there is also a good agreement between the model and data in terms of population density. The model explains 77.2% of the two-dimensional variance in population density, and 95.9% of the uni-dimensional variance. Similarly, Fig. 3(a) shows a reasonable agreement in terms of dwelling size, even though we have little data on this aspect. Finally, Fig. 3(b) shows that this agreement holds over time, at least since the 1980's.

Model and data seem to match well on the urban area scale, even if local differences can be large, due to the lack of several locally-important characteristics (e.g., public services supply and local amenities).

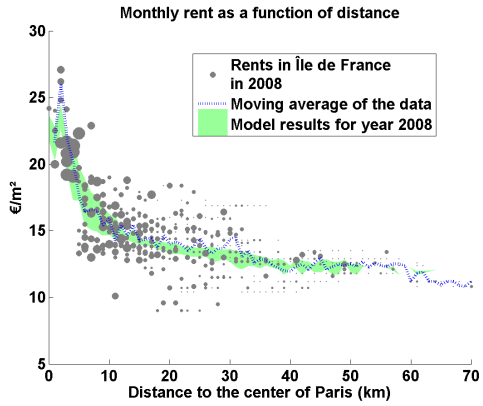
4. Scenario hypotheses

4.1. World evolution scenarios

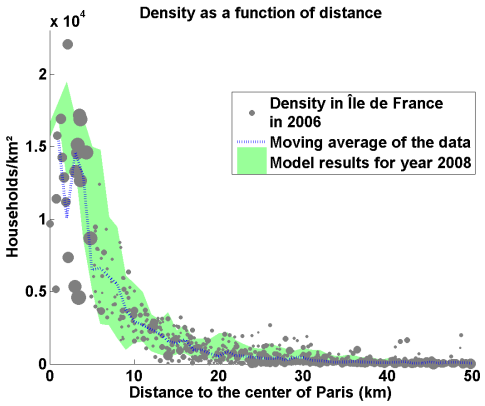
We use a set of four contrasted scenarios on world evolutions, based on several hypotheses on world population growth, fossil fuel reserves, technology availability and climate policies (Fig. 4). These hypotheses are used as input by the Imaclim-R model ([47]) to compute coherent quantitative techno-economic global scenarios on income, transport prices and technologies over the 2010-2100 period.

Imaclim-R is a global hybrid general equilibrium model with endogeneous technical change. It represents the world economy, disaggregated into 12 regions and 12 sectors. The model is hybrid in the sense that it combines macroeconomic consistency with technology explicitness. Moreover, this framework encompasses second-best features: the possible underutilization of production factors (labour and capital), the interplay between technological inertia and imperfect foresight (the price signals incorporated in adaptive expectations is a function of current

[10]For instance, bus and tramway networks are not modeled, whereas they were of great importance at the beginning of the 20th century.

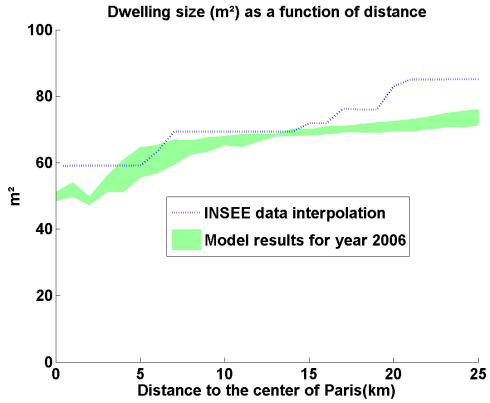


(a) Rents (Data source: CLAMEUR). The model explains 55.1% of the two-dimensional variance of the data.

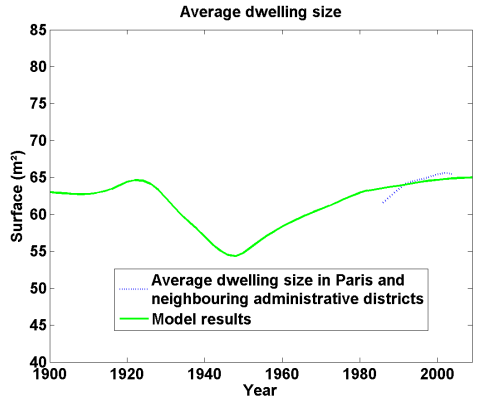


(b) Population density (Data source: INSEE). The model explains 74.7% of the two-dimensional variance of the data.

Figure 2: Rents and population density computed by the model (green area) and from data. Dots represent data for individual localities. The dotted line represents the average value of data at a given distance from Paris center.



(a) Dwelling size in 2006 (Data source: INSEE and IAU)



(b) Average dwelling size evolution (Data source: INSEE and IAU)

Figure 3: Dwelling size computed by the model (plain line) and from data.

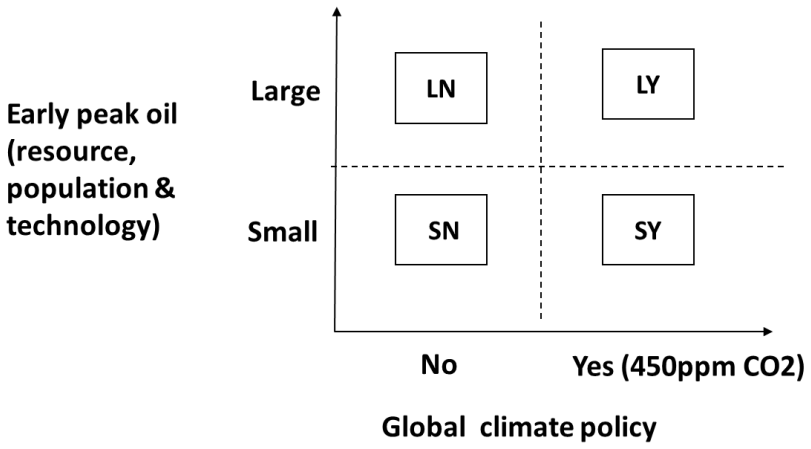


Figure 4: Global techno-economic scenarios

prices and past trends), and the rigidities of labor markets. It simulates for instance energy prices, technology market penetrations, energy production, and transport technology prices.

Main determinants of these variables include future fossil fuel availability and future climate policies. The four scenarios were computed by combining (1) two assumptions on future tensions on fossil fuel markets and (2) two assumptions on future world climate policies (see a detailed presentation of the model and of the scenarios in [47]; these two worlds are part of the 576 worlds designed for this article).

Assumptions on future tensions on fossil fuel markets result from a combinaison of hypothesis on exogenous parameters of the model describing natural resources, technologies and international economic trends. They include parameters describing oil and gas markets, the Middle-East strategy, coal markets, the availability of alternative liquid fuel supply, carbon free options for power generation and end-use technologies, and development patterns.

These parameters have been combined to maximize the difference in energy and transport prices in 2050 in these two worlds. In scenarios LN and LY (cf. Fig. 4), fossil fuels are largely available until 2040 (for instance the amount of ultimately recoverable oil resources is 3.6 Tb) while demand is high and locked in carbon-intensive pathways (development pathways are energy-intensive and the potential for low-carbon technologies is low; for instance electric vehicles cannot significantly penetrate the market). In scenarios SN and SY, the peak oil happens before 2030 (the amount of ultimately recoverable oil resources is 3.1 Tb) while the potential for low-carbon technologies is high (e.g. electric vehicles can penetrate the market as soon as 2010) and demand is less carbon-intensive. Appendix D gives a full description of all parameters values used in these two assumptions.

For climate policies, the model simulates either (i) a "Business As Usual" (BAU) world with no constraint on emissions (scenarios SN and LN), or (ii) a "stabilization" world in which a global carbon price reduces emissions such that CO_2 concentration is stabilized at 450 ppm in

the long run (corresponding to a 550 ppm CO_2eq. stabilization)(scenarios LY and SY).

Figure 6 shows some variables of the resulting techno-economic scenarios, and Fig. 5 shows the associated oil prices and carbon tax[11]. Imaclim-R computes the evolution of vehicles usage costs. In our scenarios, we suppose that public transport prices evolve proportionally to public transport usage cost, i.e. that the fraction of subsidy in public transport cost remains constant.

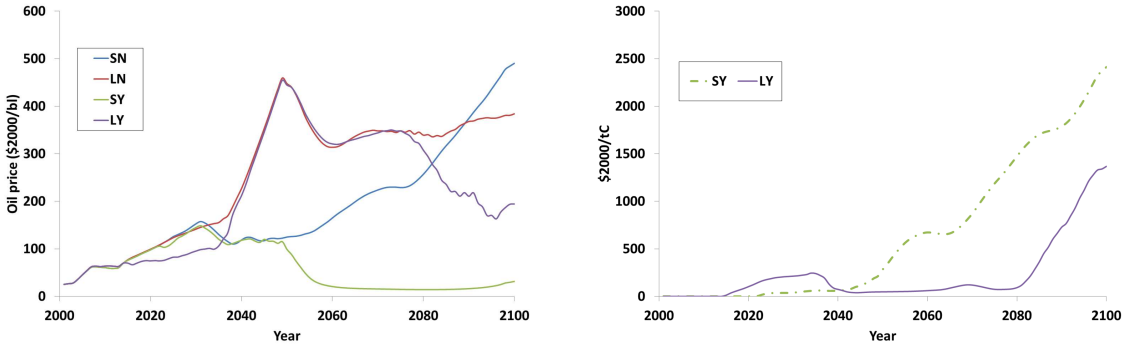
In the Imaclim-R model the oil price is endogenous. As the model is calibrated on the 2001 GTAP database and disregards some of the mechanisms driving market oil price (especially geopolitical tensions, the impact of changes in exchange rates, and market speculation), the steep increase of oil prices which happened before 2008 is not reproduced, and the oil price remains around 80$/bl until 2015 (see Fig. 5(a)).

In techno-economic scenarios LN and LY, fossil fuels are largely available until 2040, and there is a limited potential for low-carbon technologies. The large availability of oil maintains low prices for the first thirteen years of the projected period. Then, a steep twenty-year-long surge in oil prices begins just before oil production starts to decrease (i.e., before the peak oil; see Fig. 5(a)) and brings the oil price up to 450$/bl. This surge is triggered by a tension between high demand, which cannot be reduced overnight, and constraints on the deployment of oil substitutes (e.g. vehicles electrification). This is the logical outcome of a small potential for low-carbon technologies combined with low energy prices in the first period. These low prices (a) induce intensive energy consumption, (b) cause faster exhaustion and a sharper decline of conventional oil, and (c) deter investment in non-conventional production capacities and limit their availability in the post-Peak Oil period. From 2040 on, the surge in oil prices is sufficient to trigger energy efficiency and technical change towards low-carbon technologies, so that oil demand starts declining and the oil price goes back down to around 350$/bl. In scenario LY, this technical change is sufficient to meet the climate target with a relatively low carbon tax until 2080. After 2080 though, the climate target becomes more stringent and the carbon tax has to increase steeply so as to tackle the most inert sectors of the Imaclim-R model (see Fig. 5(b)). As a consequence, the oil price drops to about 200$/bl because oil demand decreases in the transportation sector.

The steep increase in oil price between 2040 and 2080, in scenarios LN and LY, is translated into the cost of private vehicles transport and public transport (see Fig. 6), but to a lesser extent. This is due to a rapid turnover in the stock of private vehicles, which can be replaced in ten years by more efficient vehicles and hybrids, and to the fact that public transports include a large part of electric technologies.

In techno-economic scenarios SN and SY, a weak Peak oil happens before 2030 and the potential for low-carbon technologies is high. In that case, oil demand is lower in the short-run than in scenarios LN and LY, preventing a strong peak oil in the 2040's. But from 2040 on, oil price increases continuously in scenario SN, until it reaches 500$/bl in 2100 (see Fig. 5(a)).

[11] Oil prices and carbon tax are not directly used as inputs by NEDUM-2D. Only transport prices for individual car and public transport (Fig. 6(a) and 6(b)), income evolution (Fig. 6(c)) and average vehicle fuel consumption (Fig. 13(d)) are used in our simulations.



(a) Oil price (excluding carbon tax).

(b) Carbon tax in scenarios SY and LY.

Figure 5: Oil price and carbon tax computed by Imaclim-R model in the four scenarios. The carbon tax is applied everywhere around the world, and is computed so that CO_2 concentration is stabilized at 450 ppm in the long run (corresponding to a 550 ppm CO_2eq. stabilization). There is no carbon tax in Techno-economic scenarios SN and LN.

This regular increase is due to the decrease in oil production, combined with high potential for technical change towards low-carbon technologies. This high potential prevents the economies from being locked in very oil-intensive technologies (as in scenario LN), so that there is no surge in oil price when Peak Oil is reached. However this regular increase in oil price is not sufficient to meet the climate target, so in scenario SY the carbon tax rises sharply to tackle the most inert sectors of the model (see Fig. 5(b)). As a consequence of this high carbon price, the oil price falls below 50$/bl after 2060 in this scenario.

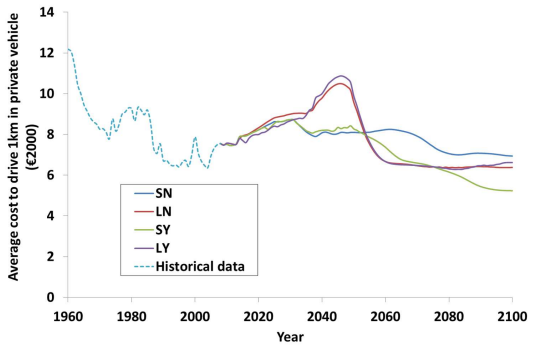
The high potential for decarbonisation in the scenarios SN and SY (e.g. in terms of electrification of vehicles) is translated into constant costs for private and public transportation in scenario SN, and a decreasing cost in scenario SY (see Fig. 6). This decreasing cost is due to a high penetration of electric vehicles in the park, as well as electricity decarbonisation, which are triggered by the carbon tax sharp and regular increase.

In these four scenarios, private vehicle usage cost per km, public transport usage cost per km and household income simulated by Imaclim-R model for the "Europe" region are used to drive NEDUM model simulations (for more information, Appendix C details the link between the data emerging from Imaclim-R model and the NEDUM-2D model).

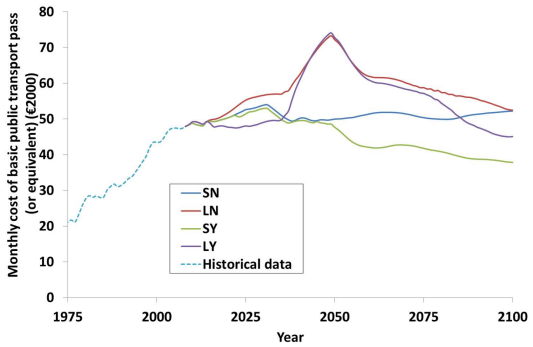
4.2. Local scenarios

These global inputs are not sufficient to create local-scale scenarios, which depend on many other factors. In particular, several local inputs are also needed.

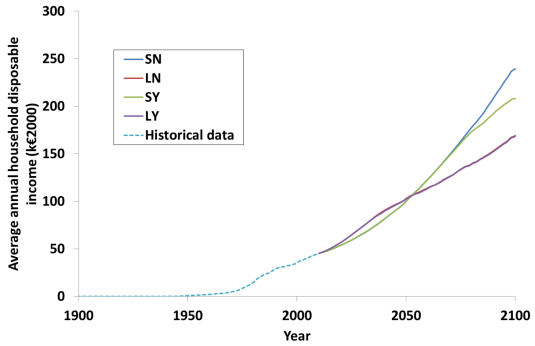
Paris urban area population evolution and households size. As inputs for population evolution and households size, we used two demographic scenarios (Fig. 7). The Low one is based, for the 2010-2030 period, on a scenario produced by the French national statistical institute (INSEE) and by the urbanism institute of Ile de France (IAU) for Paris urban area ([49]). For



(a) Average cost to drive 1km in private vehicle, including electric vehicles and carbon tax (Source for historical data: F. Nadaud ([48]), after CPDP)



(b) Monthly cost of basic public transport pass (or equivalent), including carbon tax (Source for historical data: F. Nadaud ([48]), after RATP)



(c) Average annual household disposable income. The curves for scenarios SY and LY are almost identical. Source for historical data: J. Friggit, CGEDD after INSEE*.

Figure 6: Example of inputs from Imaclim-R model. Scenarios SN and SY represent a world with high resilience against fossil fuel tensions. Scenarios LN and LY represent a world with high peak oil, happening in 2040. Scenarios SN and LN represent a world without any global climatic policy, contrary to scenarios LY and SY.

*Series downloadable on
www.cgedd.developpement-durable.gouv.fr/rubrique.php3?id_rubrique=138.

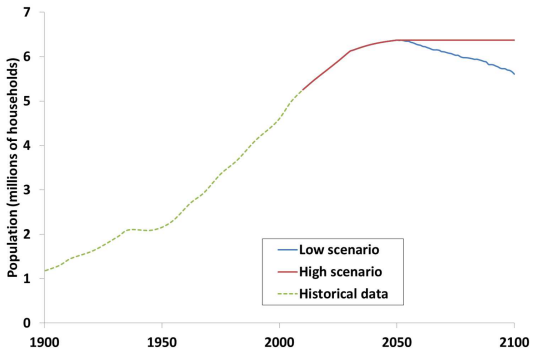


Figure 7: Demographic scenarios : number of households in Paris urban area. Source for historical data: INSEE.

the 2030-2050 period, it is based on a scenario produced by INSEE for France ([50]), and for the 2050-2100 period by a scenario produced by the UN for Europe ([51]). The High scenario is the same as the Low scenario until 2050, and is then constant.

Development of transport infrastructure. Many different assumptions about the future development of transport infrastructure can be tested with the model. For simplicity, we suppose here that infrastructure pattern remains unchanged between 2010 and 2100, and that congestion on roads and public transport remains at current levels, i.e. future investments in the transportation network are assumed to maintain the same service level in spite of population growth, without developing new lines.

Urbanism policies. We use four different scenarios for local urban policies. In the first one, we suppose that the extension of the city is entirely guided by the market: we introduce no policy or regulation limiting the extension of the city or preferentially developing certain areas. The idea is to study the "natural" trend of development of the city; this trend does not necessarily match the development that will occur in practice, but it allows understanding and anticipating land pressures, and therefore future local challenges.

In the second one, we suppose that an efficient “Green Belt policy” is enacted in 2020 to control urban sprawl and protect natural areas and agriculture activity. From that year on, building is only possible through a densification of existing built spaces, but is prohibited elsewhere.

In the third one, we suppose that a zoning policy to reduce the risk of flooding is implemented in 2020. This policy prohibits new constructions in flood-prone areas, but do not act on existing buildings.

Finally, in the fourth one, we suppose that both a flood-risk zoning policy and a green-belt policy are implemented together, in a policy that combines adaptation and mitigation objectives.

5. Results

Model results can be analyzed in view of three policy goals: reducing urban sprawl, mitigating climate change, and adapting to it.

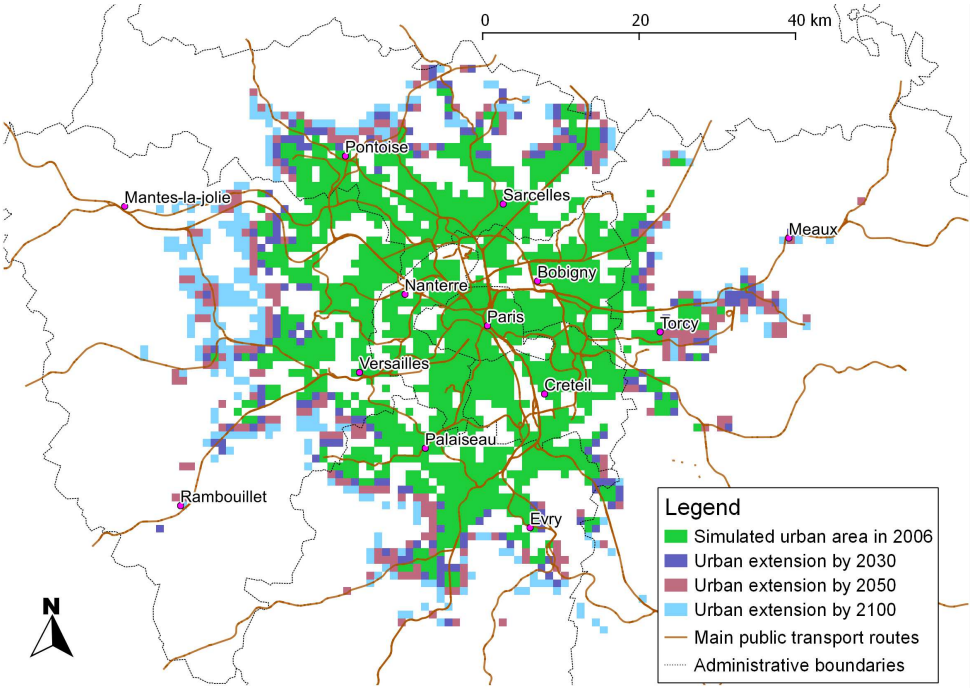


Figure 8: Example of simulated urban area extension, using techno-economic scenario SN and high demographic scenario.

5.1. Urban sprawl

Figure 8 presents an example of projected Paris urban area extension between 2010 and 2100. This example corresponds to a techno-economic scenario with a limited and early peak oil, no global climate policy to curb world greenhouse gas emissions (techno-economic scenario SN) and a demographic scenario where Paris urban area population grows until 2050, and then remains constant (high demographic scenario). In this scenario, Paris urban area expands greatly, especially between 2010 and 2030.

Changing these hypotheses changes the simulated expansion, but all factors do not have the same impact. Figure 9 shows a simulation with the same techno-economic hypotheses, but with a decreasing population between 2050 and 2100 (the low demographic scenario). In this case, some urban locations are abandonned (which could lead to city management problems, as observed for instance in eastern european shrinking cities, see Bontje [52]). However, other locations continue to be developped between 2050 and 2100, in spite of the decrease in population. This is due to the decrease in transport costs relative to income, and the subsequent population density decrease.

Techno-economic considerations seem to affect only moderately urban sprawl when compared with the impact of urbanism policies, and population changes (see Fig. 10). Even the presence of a carbon tax (at the value needed to stabilize CO2 concentration at 450 ppm, i.e. about $1000) does not influence significantly urban sprawl.

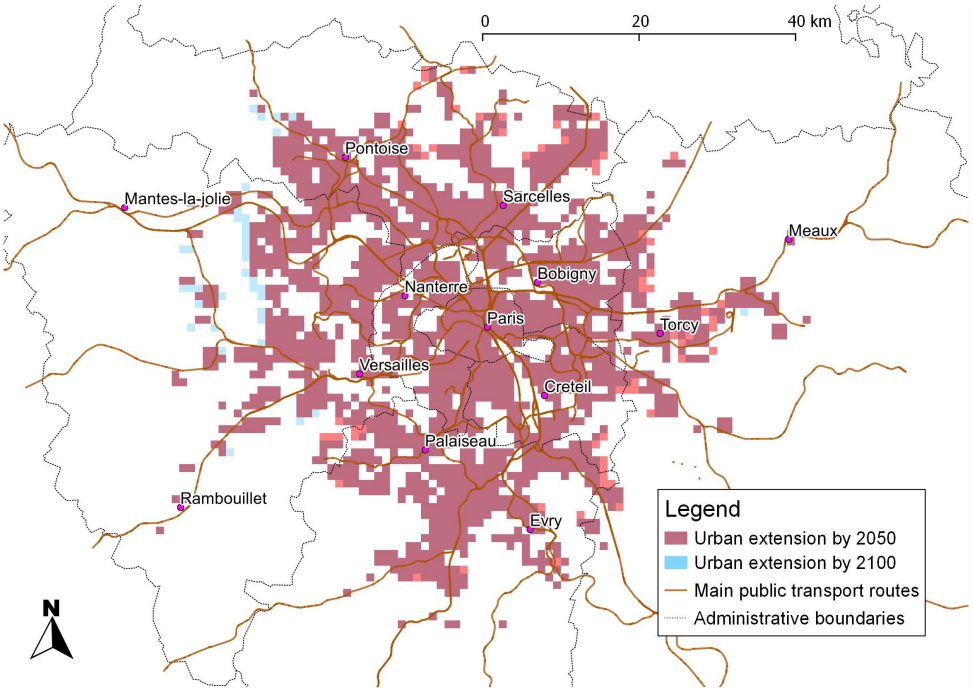


Figure 9: Example of simulated urban area extension, using techno-economic scenario SN and low demographic scenario.

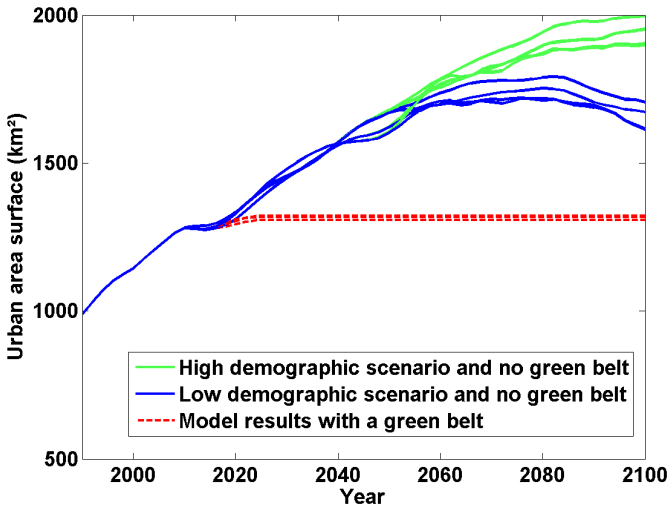


Figure 10: Urban area extension as simulated by NEDUM-2D. Plain green curves correspond to scenarios with a high population (for the four global scenarios), and blue ones to scenarios with low population, with no green belt policy in both cases. The dashed curve correspond to scenarios with the green belt policy.

This result has two origins. Firstly, it is caused by our world scenarios: in these scenarios, an important "peak oil" and a high carbon tax impact moderately transport prices (the maximum increase is about 20%) , because they are compensated by vehicle energy consumption decrease and alternative energy use (especially electric vehicles and decarbonized electricity in the case of scenarios with a climate policy and liquefied coal in the other scenarios).

Secondly, in our model, households respond to a generalized cost of transport, which is the sum of the actual monetary cost of transportation, plus a cost associated to travel time. To compute the latter, as explained in Section 3.2, we use a cost of time which increases proportionally to households income. In all the simulations computed by the Imaclim-R model, households income increases strongly (almost exponentially) over time (Fig. 6(c)), whereas transport monetary cost increases only moderately (Fig. 6(a) and 6(b)). Therefore, in all scenarios, transport monetary cost becomes gradually negligible compared to transport time cost (Tab. 1). As transportation times are the same in all our scenarios, the differences between scenarios tend to decrease.

Year	**2010**	**2050**	**2100**
Monetary cost (€2000)	1,070	1,210	1,150
Fraction of generalized cost	*9.79%*	*5.31%*	*2.15%*
Time cost cost (€2000)	9,870	21,580	52,240
Fraction of generalized cost	*90.21%*	*94.69%*	*97.85%*

Table 1: Comparison between transport monetary cost and cost associated to transport time, in average, 20km from the center of Paris. Cost associated to transport time appears to be about 10 times higher than transport monetary cost in 2010. This ratio increases over time.

As highlighted in Section 3.1, there are some empirical and theoretical evidences that time cost may not evolve proportionally to income , because of technological innovations that make travel more comfortable.[12] The elasticity of time cost relative to income variation may be as low as 0.5 ([46]). But it should be noted that, even in this case, in the simulations, costs associated with transportation times increase much more over the century than monetary transport costs, and that urban sprawl remains marginally impacted by energy prices.

This result suggests especially that climate policies based on a carbon price aiming at limiting global emissions would only have a marginal impact on urban forms. Other policies are needed to slow down urban sprawl. Examples of these policies include specific land-use policies (urban planning regulations such as the green belt policy modelled here, but also other policies such as local taxes), or direct investments in transport which would change travel times across the urban area. This result is consistent with Viguié and Hallegatte [29], which concluded that a 100€/tC carbon tax alone seemed unsufficient to mitigate urban sprawl.

[12] It may also seem reasonable to imagine a scenario where an increasing transport congestion would make travel less comfortable. In such a scenario, time cost would increase more rapidly than income.

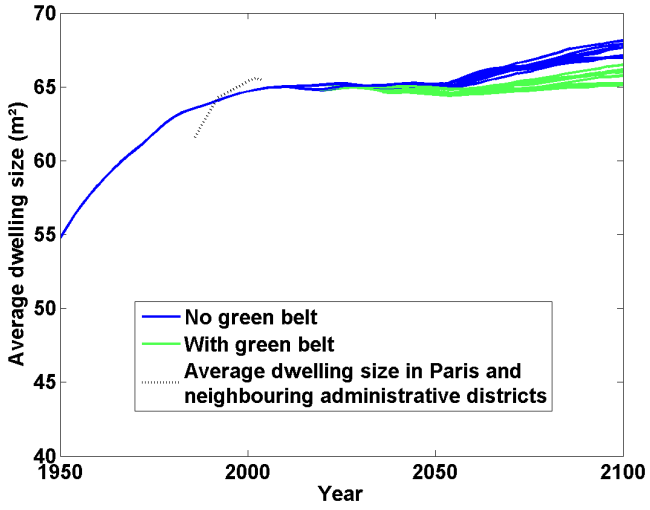


Figure 11: Average dwelling size evolution. Green curves correspond to scenarios with a high population, and blue ones to scenarios with low population. The dotted black line corresponds to actual historic data (Source : INSEE and IAU).

Of course, techno-economic scenarios with a lower income growth, or even with an income stagnation or decrease could lead to different conclusions.

5.2. Mitigation

All scenarios predict a growth in dwelling size, coherent with historical trends (Fig. 11). This growth appears to be mainly impacted by the existence or not of a greenbelt policy: when such a policy is implemented, increased land scarcity leads to an increase in real estate prices, and hence to smaller dwellings[13]. However, in all scenarios, transport cost decreases relatively to income. This enables people to locate more and more uniformly in the urban area (Section 2), thus reducing real estate pressure, and counterbalancing the former mechanism. Consequently, even when a greenbelt policy is implemented, dwelling size appears to increase over time (although less quickly than when no green belt policy is implemented). Such an increase could have an impact on greenhouse gases emissions, through an increase in energy consumption for heating or cooling.

The green belt enables also to mitigate public transport modal share decrease (Fig. 12). However, it does not appear sufficient to prevent this decrease, which happens for all scenarios.

As shown in Fig. 13, if transport-related emissions are impacted by many variables, the main influence comes from techno-economic scenarios, i.e. fuel prices and transport technologies

[13] In practice, this could also lead to a reduced city attractivity, and therefore to a smaller population than in the scenarios with no greenbelt policy (in the line of [53]). This could indirectly impact average dwelling size. In our simulations, demographic scenarios are exogeneous, so we could not study such phenomena.

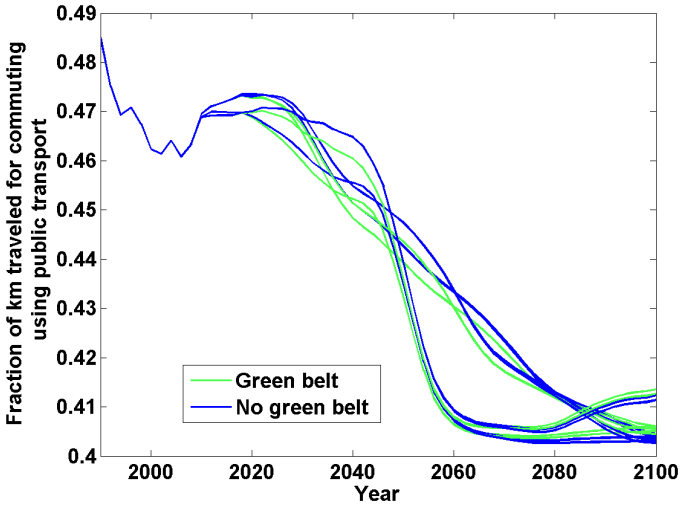


Figure 12: Public transport modal share for commuting trips. Actual data for 2002 is 46.63 % (Source : DREIF).

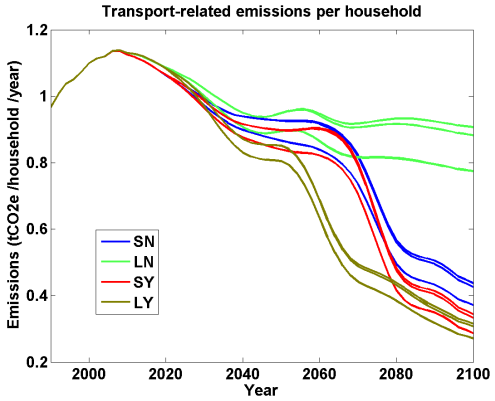
evolution. The average distance traveled using private car (strongly related in our modelling to city sprawl) is greatly impacted by the implementation of a greenbelt policy, because of a modal shift towards public transport[14], and because of the reduced length of trips. However, in terms of greenhouse gases emissions, this has a much lower effect that the variation in vehicle efficiency and technology from the socio-economic scenario (e.g. availability of electric vehicles and decarbonized electricity).

In our downscaled scenarios, therefore, transport-related greenhouse gas emissions in the city are mainly driven by technologies. With the urban policies we have tested, urban planning plays a limited role in spite of its influence on the distance traveled by car. It means that if technologies cannot contribute to emission reductions, then limiting emissions from urban transportation would require the implementation of urban planning options that are much stricter than what has been investigated in this article. In practice, since a green belft would not be sufficient, it means that *urban reconstruction*, i.e. a combination of building destruction and construction, would become necessary.

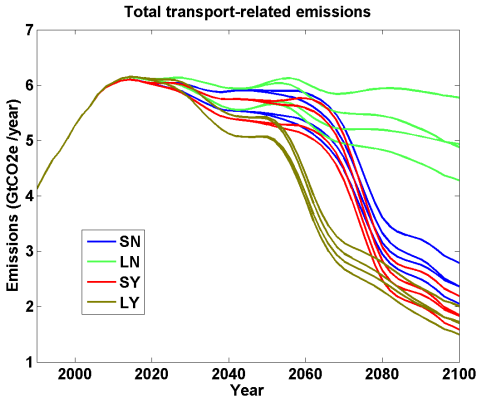
5.3. Adaptation

These scenarios are also useful for climate change adaptation and vulnerability analyzes ([54]). In Paris, one of the main disaster risks is flooding, and climate change may increase this risk, even though models still disagree. Figure 14 shows how population living in flood-

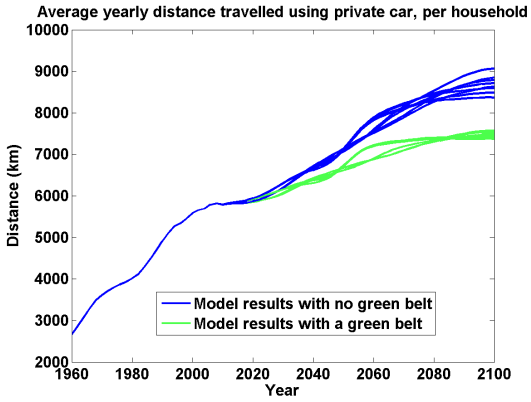
[14]The densification of the urban area makes a larger fraction of the inhabitants live close to public transport stations.



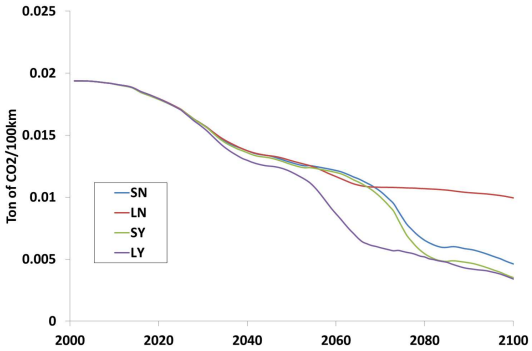
(a) Transport-related emissions per household



(b) Total transport-related emissions



(c) Average yearly distance traveled using private car,per household



(d) Average private vehicle emissions per passenger-km. Average over all circulating private cars. Public transport emissions are much smaller, about 4.10^{-4} tCO2/100km or less in all scenarios.

Figure 13: Transport-related emissions.

prone areas[15] can be expected to evolve in the future. This data is an essential input to assess how changes in rainfall may translate into flood losses, and therefore to assess climate change impacts. The simulated population living in flood-prone areas is consistent with observations (empirical estimations for 1999 and 2006 are presented on Fig. 14). In all scenarios, this population increases until 2030 before decreasing slowly. This decrease is related to a diminishing population density in risk zones.

It should be noted that a greenbelt policy appears to increase the number of households living in flood-prone areas (Fig. 14(a)), because it increases population density in flood-prone area. Such a phenomenon has been observed empirically by Burby et al. [55] and Lall and Deichmann [56]. This negative side-effect should be balanced with the positive effect on urban sprawl and transport demand (see [30], for a more detailed study of such trade-offs).

This conclusion is true even when a flood-risk zoning is implemented (Fig. 14(b)), i.e. even when new buildings in flood-exposed zones are forbidden. Indeed, we suppose here that this policy prevents new buildings in places not already urbanized, but does not prevent densification in places already built. As explained in Section 5.2, dwelling size is smaller when a greenbelt policy is implemented, and more people are therefore living in flood-risk zones in these scenarios.

As can be seen on Fig. 14(b), the "flood risk zoning policy" that we have considered here has a weak impact on flood risk, when compared to other variables. Here, again, as for mitigation, urban planning plays a limited role, and to reach a significant impact it requires strong measure going beyond what is usually done ([57]).

Heat wave vulnerability is another important topic strongly related to urban extension. To investigate this topic, three on-going research projects[16] are coupling this urban model with the urban microclimate model TEB ([58]).

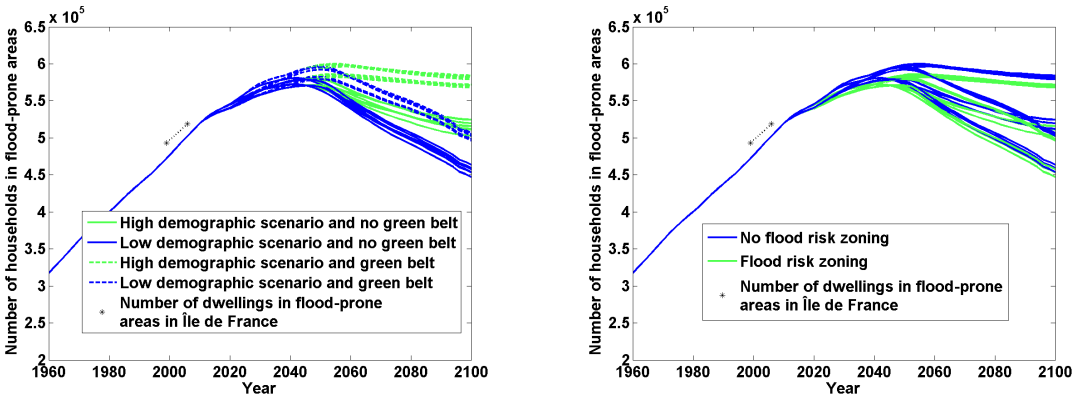
6. Conclusion

NEDUM-2D captures the main long-term determinants of city evolution; it is able to reproduce the main tendencies of past Paris urban area evolution. From global socio-economic scenarios, it enables to derive local scenarios for the Paris urban area. These scenarios appear useful to support decision-making about urban sprawl, emissions reduction policies and climate change adaptation.

The main conclusions of this study are not the quantitative figures computed in the scenarios, but the relative orders of magnitude and the qualitative reasons explaining them (tab. C.1 sums up key results). Firstly, transport price considerations seem to affect only moderately urban

[15] We used present-day flood-prone areas (Source: CARTO RISQUE, French Ministry of environment MEDDTL). This analysis could be made more refined by coupling the urban model with an hydrological model to take into account the impacts of climate change on the frequency and intensity of floods.

[16] VURCA, MUSCADE and ACCLIMAT projects (http://www.cnrm.meteo.fr/ville.climat/?lang=en).



(a) Green curves correspond to scenarios with a high population, and blue ones to scenarios with low population. Dotted lines correspond to scenarios with no green belt policy, and plain ones to scenarios with a green belt policy.

(b) Green curves correspond to scenarios with flood risk zoning, and blue ones to scenarios without.

Figure 14: Number of households living in flood-prone areas, as simulated by NEDUM-2D. The dotted black line corresponds to actual historic data (Source: French Ministry of environment MEDDTL (CGDD/SOeS), after Corine Land Cover and CARTO RISQUE databases).

	Urban sprawl	Mitigation	Adaptation (flood risk)
Population change	H	l	H
Urban containment policy	H	l	H
Techno-economic scenarios (transport prices and technologies)	l	H	l
Flood risk zoning	l	l	l

Table 2: Main conclusions: impact of variables on main objectives. H stands for pour "high impact" and l for "low impact". The "flood risk zoning policy" that we have considered here does not prevent densification in places already urbanized. It has therefore a weak impact on flood risk, when compared to other variables.

sprawl when compared with the impact of population changes and urbanism policies. Even the presence of a carbon tax (at the value needed to stabilize CO2 concentration at 450 ppm) does not influence it significantly. In other words, possible future increases in fuel prices seem insufficient to slow suburbanization, and other measures are needed if one wants to slow down urban sprawl. Examples of these measures include specific land-use policies (urban planning regulations, local taxes), or direct investments in transport infrastructure.

A second conclusion is that, conversely, techno-economic scenarios (and especially vehicle efficiency) play the major role concerning commuting transport-related greenhouse gases emissions. The reason behind that is, that, in all scenarios, the variation in transport demand, when demography changes or when a green belt policy is implemented, appears to be smaller than the expected variation in vehicle efficiency. Only a much stricter anti-sprawl urbanism policy or much more contrasted demographic scenarios would ultimately be able to change this conclusion. One important consequence of this result is that the urban policies needed to limit emissions from urban transportation are highly dependent on the technologies that will eventually be available. If technology is unable to achieve sufficient emissions control, then very strict constraints on urban development, more than the green belt policy tested here, will be necessary. A re-engineering of the city, its buildings and infrastructure may even be required.

The third conclusion is about climate change adaptation: concerning flood-risk, the population living in flood-prone areas increases in all scenarios until 2030, before decreasing slowly. This decrease is related to a diminishing population density in risk zones. A greenbelt policy appears to increase the number of households living in flood-prone areas, because it increases the population density. This is true even when a flood-risk zoning is implemented, i.e. when new building in flood-exposed zones is forbidden.

As our modeling is monocentric, it was not possible to simulate the effect of an increased development of other subcenters in the urban area. Such a development would result in alternative scenarios. However, the mechanisms leading to the main conclusions of this paper do not depend on the city being monocentric or not, and should remain valid in a polycentric setting. A more complex, polycentric model is under development and will be useful to test the influence of other new variables, and especially investment in services supply (schools, health, leisure...) across the urban area.

Techno-economic scenarios with a lower income growth, or even with an income stagnation or decrease could lead to different conclusions. We have only downscaled a small number of scenarios in this study : to assess the robustness of the former results, other scenarios should be downscaled. More systematic exploration of the impact of the variation of global scenarios is also an important part of our research agenda.

Acknowledgements

This study benefited from funding by the Agence Nationale de la Rercherche through the projects “Vulnérabilité Urbaine aux épisodes Caniculaires et stratégies d’Adaptation” (VURCA) (ANR-08-VULN-013) and “Modélisation Urbaine et Stratégies d’adaptation au Changement

climatique pour Anticiper la Demande et la production Energétique" (MUSCADE) (ANR-09-VILL-0003-01) projects.

The authors are grateful to Didier Rouchaud, Alain Sauvant, Jean-Luc Salagnac, and Nicolas Coulombel for providing invaluable data. Adrien Vogt-Schilb and Paolo Avner provided helpful comments.

The findings, interpretations, and conclusions expressed in this paper are entirely those of the authors. They do not necessarily represent the views of the International Bank for Reconstruction and Development/World Bank and its affiliated organizations or those of the executive directors of the World Bank or the governments they represent.

References

[1] D. Dodman, Blaming cities for climate change? an analysis of urban greenhouse gas emissions inventories, Environment and Urbanization 21 (2009) 185–201.

[2] C. Rosenzweig, W. Solecki, S. A. Hammer, S. Mehrotra, Cities lead the way in climate-change action, Nature 467 (2010) 909–911.

[3] D. Hoornweg, L. Sugar, C. L. T. Gomez, Cities and greenhouse gas emissions: moving forward, Environment and Urbanization 23 (2011) 207–227.

[4] R. J. Dawson, J. W. Hall, S. Barr, M. Batty, A. Bristow, S. Carney, S. Evans, A. Ford, J. Köhler, M. Tight, et al., A blueprint for the integrated assessment of climate change in cities, Working Paper 104, Tyndall Centre for Climate Change Research, 2007.

[5] S. Hallegatte, J. Corfee-Morlot, Understanding climate change impacts, vulnerability and adaptation at city scale: an introduction, Climatic Change 104 (2010) 1–12.

[6] A. Revi, Climate change risk: an adaptation and mitigation agenda for indian cities, Environment and Urbanization 20 (2008) 207.

[7] F. Gusdorf, S. Hallegatte, Behaviors and housing inertia are key factors in determining the consequences of a shock in transportation costs, Energy Policy 35 (2007) 3483–3495.

[8] F. Gusdorf, S. Hallegatte, A. Lahellec, Time and space matter: How urban transitions create inequality, Global Environmental Change 18 (2008) 708–719.

[9] W. D. Solecki, C. Oliveri, Downscaling climate change scenarios in an urban land use change model, Journal of Environmental Management 72 (2004) 105–115.

[10] S. R. Gaffin, C. Rosenzweig, X. Xing, G. Yetman, Downscaling and geo-spatial gridding of socio-economic projections from the IPCC special report on emissions scenarios (SRES), Global Environmental Change Part A 14 (2004) 105–123.

[11] R. Matthias, D. Coelho, Understanding and managing the complexity of urban systems under climate change, Climate Policy 7 (2007) 317–336.

[12] A. Grübler, B. O'Neill, K. Riahi, V. Chirkov, A. Goujon, P. Kolp, I. Prommer, S. Scherbov, E. Slentoe, Regional, national, and spatially explicit scenarios of demographic and economic change based on SRES, Technological Forecasting and Social Change 74 (2007) 980–1029.

[13] E. Kriegler, B. C. O'Neill, S. Hallegatte, T. Kram, R. Lempert, R. H. Moss, T. J. Wilbanks, Socio-economic Scenario Development for Climate Change Analysis, Technical Report, CIRED Working Paper DT/WP, 2010.

[14] D. P. Van Vuuren, K. Riahi, R. Moss, A. Thomson, N. Nakicenovic, J. Edmonds, T. Kram, F. Berkhout, R. Swart, Developing new scenarios as a thread for future climate research, Technical Report, IPCC, 2010.

[15] R. J. Lempert, Shaping the next one hundred years: new methods for quantitative, long-term policy analysis, Rand Corporation, 2003. URL: http://books.google.com/books?hl=fr&lr=&id=lKZOGEenGFQC&oi=fnd&pg=PP1&dq=Shaping+the+Next+100+Years:+New+Methods+for+Quantitative,+Long-Term+Policy+Analysis&ots=KukOOTMYYm&sig=MX1JB5TRxPrOs_909oIFNiQ8RXc.

[16] I. P. Holman, M. D. A. Rounsevell, S. Shackley, P. A. Harrison, R. J. Nicholls, P. M. Berry, E. Audsley, A regional, multi-sectoral and integrated assessment of the impacts of climate and socio-economic change in the uk: Part i. methodology, Climatic Change 71 (2005) 9–41.

[17] R. J. Dawson, T. Ball, J. Werritty, A. Werritty, J. W. Hall, N. Roche, Assessing the effectiveness of non-structural flood management measures in the thames estuary under conditions of socio-economic and environmental change, Global Environmental Change 21 (2011) 628–646.

[18] C. L. Walsh, R. J. Dawson, J. W. Hall, S. L. Barr, M. Batty, A. L. Bristow, S. Carney, A. S. Dagoumas, A. C. Ford, C. Harpham, et al., Assessment of climate change mitigation and adaptation in cities, Proceedings of the ICE-Urban Design and Planning 164 (2011) 75–84.

[19] M. Mokrech, R. J. Nicholls, R. J. Dawson, Scenarios of future built environment for coastal risk assessment of climate change using a GIS-based multicriteria analysis, Environment and Planning B: Planning and Design 39 (2012) 120–136.

[20] B. Lefevre, Long-term energy consumptions of urban transportation: A prospective simulation of, Energy Policy 37 (2009) 940–953.

[21] C. M. Fontaine, M. D. A. Rounsevell, An agent-based approach to model future residential pressure on a regional landscape, Landscape Ecology 24 (2009) 1237–1254.

[22] D. Haase, N. Schwarz, Simulation models on Human Nature interactions in urban landscapes: A review including spatial economics, system dynamics, cellular automata and agent-based approaches, Living Reviews in Landscape Research 3 (2009) 1–5.

[23] N. Nakicenovic, J. Alcamo, G. Davis, B. de Vries, J. Fenhann, S. Gaffin, K. Gregory, A. Grubler, T. Y. Jung, T. Kram, et al., Special report on emissions scenarios: a special report of Working Group III of the Intergovernmental Panel on Climate Change, Technical Report, Pacific Northwest National Laboratory, Richland, WA (US), Environmental Molecular Sciences Laboratory (US), 2000.

[24] A. Grübler, N. Nakicenovic, K. Riahi, F. Wagner, G. Fischer, I. Keppo, M. Obersteiner, B. O'Neill, S. Rao, F. Tubiello, Integrated assessment of uncertainties in greenhouse gas emissions and their mitigation: Introduction and overview, Technological Forecasting and Social Change 74 (2007) 873–886.

[25] P. H. Verburg, P. P. Schot, M. J. Dijst, A. Veldkamp, Land use change modelling: current practice and research priorities, GeoJournal 61 (2004) 309–324.

[26] M. K. Jat, P. Garg, D. Khare, Monitoring and modelling of urban sprawl using remote sensing and GIS techniques, International Journal of Applied Earth Observation and Geoinformation 10 (2008) 26–43.

[27] M. Iacono, D. Levinson, A. El-Geneidy, Models of transportation and land use change: a guide to the territory, Journal of Planning Literature 22 (2008) 323–340.

[28] F. Gusdorf, S. Hallegatte, Compact or spread-out cities: Urban planning, taxation, and the vulnerability to transportation shocks, Energy Policy 35 (2007) 4826–4838.

[29] V. Viguié, S. Hallegatte, The impact of a carbon tax on paris metropolitan area and its population, submitted (2011).

[30] V. Viguié, S. Hallegatte, Trade-Offs and synergies in urban climate policies, Nature Climate Change 2 (2012) 334–337.

[31] V. Viguié, Urban dynamics modelling, application to economic assessment of climate change, Ph.D. thesis, CIRED, Ecole des Ponts ParisTech, Université Paris Est, Paris, France, 2012.

[32] W. Alonso, Location and land use: toward a general theory of land rent, Harvard University Press, Cambridge, MA, 1964.

[33] E. S. Mills, An aggregative model of resource allocation in a metropolitan area, The American Economic Review 57 (1967) 197–210.

[34] R. F. Muth, Cities and Housing; the Spatial Pattern of Urban Residential Land Use, University of Chicago Press, Chicago, 1969.

[35] M. Fujita, Urban Economic Theory: Land Use and City Size, Cambridge University Press, Cambridge [Cambridgeshire], 1989.

[36] J. K. Brueckner, Urban general equilibrium models with non-central production, Journal of Regional Science 18 (1978) 203–215.

[37] M. Fujita, H. Ogawa, Multiple equilibria and structural transition of non-monocentric urban configurations, Regional science and urban economics 12 (1982) 161–196.

[38] A. Anas, I. Kim, General equilibrium models of polycentric urban land use with endogenous congestion and job agglomeration, Journal of Urban Economics 40 (1996) 232–256.

[39] R. E. Lucas, E. Rossi-Hansberg, On the internal structure of cities, Econometrica 70 (2002) 1445–1476.

[40] M. Berliant, S.-K. Peng, P. Wang, Production externalities and urban configuration, Journal of Economic Theory 104 (2002) 275–303.

[41] G. Giuliano, Land use impacts, of transportation investments, in: The geography of urban transportation, The Guilford Press, 2004, p. 237.

[42] W. C. Wheaton, Commuting, congestion, and employment dispersal in cities with< i> mixed</i> land use, Journal of Urban Economics 55 (2004) 417–438.

[43] R. Arnott, Congestion tolling with agglomeration externalities, Journal of Urban Economics 62 (2007) 187–203.

[44] OLS, Les attributions dans le parc social francilien en 2007, Technical Report, Observatoire du Logement Social en ï¿œle de France (Observatory of Social Housing in Ile de France), 2008.

[45] L. Zamparini, A. Reggiani, Meta-Analysis and the value of travel time savings: A transatlantic perspective in passenger transport, Networks and Spatial Economics 7 (2007) 377–396.

[46] J. D. Shires, G. C. de Jong, An international meta-analysis of values of travel time savings, Evaluation and program planning 32 (2009) 315–325.

[47] J. Rozenberg, S. Hallegatte, A. Vogt-Schilb, O. Sassi, C. Guivarch, H. Waisman, J. C. Hourcade, Climate policies as a hedge against the uncertainty on future oil supply, Climatic change 101 (2010) 663–668.

[48] F. Nadaud, J. Hourcade, Le prix du petrole, les prix des carburants et nous : un regard rï¿œtrospectif, R2DS working paper 3 (2009).

[49] P. Louchart, Près d'un million de ménages franciliens en plus á l'horizon 2030, IAU, Note rapide Société 495 (2010).

[50] I. Robert-Bobee, Projections de population pour la france metropolitaine aï¿œ l'horizon 2050, INSEE premiere 1089 (2006).

[51] United Nations, World Population Prospects, the 2010 Revision, Technical Report, United Nations, Department of Economic and Social Affairs, Population Division, New York, 2011. URL: http://esa.un.org/unpd/wpp/Excel-Data/population.htm.

[52] M. Bontje, Facing the challenge of shrinking cities in east germany: The case of leipzig, GeoJournal 61 (2005) 13–21.

[53] E. L. Glaeser, M. E. Kahn, The greenness of cities: carbon dioxide emissions and urban development, Journal of Urban Economics 67 (2010) 404–418.

[54] S. Hallegatte, V. Przyluski, A. Vogt-Schilb, Building world narratives for climate change impact, adaptation and vulnerability analyses, Nature Climate Change 1 (2011) 151–155.

[55] R. J. Burby, A. C. Nelson, D. Parker, J. Handmer, Urban containment policy and exposure to natural hazards: Is there a connection?, Journal of Environmental Planning and Management 44 (2001) 475–490.

[56] S. V. Lall, U. Deichmann, Density and Disasters, Policy Research Working papers 5161, The World Bank, Washington DC, USA, 2009.

[57] L. Faytre, Logement : quelle exposition du parc francilien en zone inondable ?, IAU, Note rapide Territoires (2013).

[58] V. Masson, A physically-based scheme for the urban energy budget in atmospheric models, Boundary-Layer Meteorology 94 (2000) 357–397.

[59] M. A. Davis, F. Ortalo-Magné, Household expenditures, wages, rents, Review of Economic Dynamics 14 (2010) 248–261.

[60] P. Thorsnes, Consistent estimates of the elasticity of substitution between land and Non-Land inputs in the production of housing, Journal of Urban Economics 42 (1997) 98–108.

[61] M. Wilhelmsson, House price depreciation rates and level of maintenance, Journal of Housing Economics 17 (2008) 88–101.

[62] D. Rouchaud, A. Sauvant, Prix des logements et coûts de transports: un modèle global d'équilibre en île-de-france., Notes de synthèses du SES. Ministère de l'équipement. (2004).

[63] J. C. Castel, Couts immobiliers et arbitrages des operateurs: un facteur explicatif de la ville diffuse, Annales de la recherche urbaine 102 (2007).

[64] M. Boiteux, L. Baumstark, Transports: choix des investissements et cout des nuisances, Rapports du Commissariat General du Plan, juin (2001).

Appendix A. Description of NEDUM-2D model

This appendix sets up the formal representation of the mechanisms described in Section 2.

Appendix A.1. Utility function

As in [29], we model the household trade-off using the following utility function:

$$U(r) = Z(r)^{\alpha} q(r)^{\beta} \tag{A.1}$$

where r is the location in the city, α and β are coefficients ($\alpha + \beta = 1$), $q(r)$ the surface of the households' dwelling and $Z(r)$ the money remaining after the household has paid its rent and a commuting round-trip per day to the center of Paris. The cost of transportation includes the monetary cost of transportation and the cost associated with the trip duration[17]. Such a functional form is consistent with the fact that the share of households' income devoted to housing expenditures is relatively constant ([59]). Households' income constraint reads:

$$Y = Z(r) + q(r) \cdot R(r) + T(r) \tag{A.2}$$

where Y is household income and is constant ($\forall r, Y(r) = Y$), $R(r)$ is the rent per square meter, and $T(r)$ transportation costs (monetary cost added with time cost).

Appendix A.2. Housing service per household

We assume that households permanently adapt their housing-service consumption to prices so as to increase their utility level to prices. Given the location r, the amount of composite goods consumed is strictly dependent on housing choices: $Z(r) = Y - T(r) - q(r) \cdot R(r)$. We have, therefore:

$$U(r) = [Y - T(r) - q(r) \cdot R(r)]^{\alpha} \cdot q(r)^{\beta} \tag{A.3}$$

Using this function, we consider that households can adjust their level of housing service consumption so as to improve their utility level : taking rent level $R(r)$ as given, households increase or decrease the size of their flats so as to maximize their utility. Adjustment in housing service consumption per capita can also include changes in the size and composition of households, for example through changes in flat-sharing practices, or changes in the age at which children leave their parents' home.

A household maximizes its utility if and only if:

- Its share of income devoted to housing service is equal to β : $q^*(r) \cdot R(r) = \beta(Y - T(r))$
- Its share of income devoted to composite good is equal to α : $Z^*(r) = \alpha(Y - T(r))$

[17] We consider the cost associated with the trip duration as an actual loss of income.

It is rational for the inhabitants to make their consumption of housing service tend to $q^*(r)$. Of course, an increase in housing consumption is authorized if and only if such an increase is physically possible, i.e. if there is available housing at this location.

Changes in flat sizes cannot happen instantaneously, for instance because it takes "time" to find a new place to live. The inertia of this mechanism is accounted for by the timescale τ_q.

Let $\Psi(r)$ be the number of unoccupied dwellings at each location :

$$\Psi(r) = H(r) - q(r) \cdot n(r) \tag{A.4}$$

The dynamics of $q(r)$ is given by :

$$\frac{dq(r)}{dt} = \begin{cases} \frac{1}{\tau_q}(q^*(r) - q(r)) = \frac{1}{\tau_q}\left(\frac{\beta(Y-T(r))}{R(r)} - q(r)\right) & \text{if } \Psi(r) > 0 \text{ or } q^*(r) < q(r) \\ 0 & \text{if } \Psi(r) = 0 \text{ and } q^*(r) > q(r) \end{cases} \tag{A.5}$$

Appendix A.3. Moving throughout the city

Households can change locations: the ones living at location r may choose to stay or move to another location. We assume they are willing to move when their local utility level $u(r)$ is under the average utility level $\bar{u}$ throughout the city: households living at locations where $u(r) \leq \bar{u}$ source are attracted to places where $u(r) \geq \bar{u}$.

Let $w(r)$ be a weighting function[18], which compares utility level $u(r)$ to $\bar{u}$. We can define :

- if $u(r) \leq \bar{u}$, $m^-(r) = w(r) \cdot n(r)$ is the number of households willing to leave
- if $u(r) \geq \bar{u}$, $m^+(r) = w(r) \cdot \Psi(r)$ is the number of attractive unoccupied dwellings

We have now to take into account city population variation. We know at every time step the population that the city should be POP_{exo} , and the population in the simulated city is POP. Let us define Δ as the difference between the two populations: $\Delta = POP_{exo} - POP$. Let us suppose now that newcomers only choose to locate in areas where utility is bigger than $\bar{u}$: the total aggregated demand of dwellings is equal to:

$$D = \int_{u(r)<\bar{u}} m^-(r)dr + \max(\Delta, 0) \tag{A.6}$$

and the aggregated supply of dwellings:

$$S = \int_{u(r)<\bar{u}} m^+(r)dr - \min(\Delta, 0) \tag{A.7}$$

[18]We have chosen $w(u) = \frac{2}{\pi}\arctan(\alpha|\frac{u-\bar{u}}{\bar{u}}|)$ where $\alpha = \frac{1}{5\%}\tan(\frac{\pi}{2}.95\%)$, so that $w(u) \geq 95\%$ when the difference between u and $\bar{u}$ is bigger than 5% of $\bar{u}$.

There is a priori no reason why the demand for moves should equal the supply of available housing. The relationships giving the moves $\mu(r)$ meet these physical constraints :

$$\mu(r) = \begin{cases} m^+(r) \cdot \min(1, D/S) & \text{if } u(r) > \overline{u} \\ m^-(r) \cdot \min(1, S/D) & \text{if } u(r) \leq \overline{u} \end{cases} \tag{A.8}$$

As for changes in flat sizes, moves of households cannot happen instantaneously. The inertia of this mechanism is accounted for by the timescale τ_n.

The number of households living at location r evolves according to the moves:

$$\frac{dn(r)}{dt} = \frac{1}{\tau_n}\mu(r) \tag{A.9}$$

Appendix A.4. Rent curve dynamics

Rent level $R(r)$ evolves in reaction to local supply and demand of housing service $H(r)$. Demand is expressed by the number of households $n(r)$ living at this location and consuming an amount of housing service $q(r)$, and by the number of households willing to move to or from this location:

- Rent level decreases if demand is lower than local supply, that is, if existing buildings are not fully occupied.
- If buildings at location r are fully occupied, rent levels increase if inhabitants want to increase their consumption of housing service, or if there are outside households willing to move to this location.

The orders of magnitude of these evolutions are determined by the relative difference between local demand and supply of housing service. Moreover, we assume that, for institutional reasons[19], housing rents do not clear the housing market instantaneously. The inertia of rent levels evolution is characterized in the model by the timescale τ_R.

Landlords decrease their rents when all dwellings are not occupied, and increase them when demand is bigger than dwelling supply. Let

$$n^*(r) = n(r) + \max(\mu(r), 0) + n_{virtual}(r) \tag{A.10}$$

be the number of households living or willing to leave at a certain location in the city. It is the sum of the number of inhabitants living at this location $n(r)$, the number of households about to move to this location $max(\mu(r), 0)$, and the number of households, $n_{virtual}(r)$, who would like to live in this location, but cannot because there are not enough available dwellings.

[19]For instance in France, when there is no tenant change, rent can only change significantly every three years.

Let us define the number of dwellings in the attractive locations by :

$$m^+_{rent}(r) = \begin{cases} w(r) \cdot \frac{H(r)}{q(r)} & \text{when } u(r) > \bar{u} \\ 0 & \text{when } u(r) \leq \bar{u} \end{cases} \tag{A.11}$$

and its aggregated sum over the whole city :

$$S_{rent} = \int_{u(r)>\bar{u}} m^+_{rent}(r)dr \tag{A.12}$$

To calculate the pressure on the housing market, we have to distribute, over the various locations, households who would like to move but cannot. We spread them over all attractive locations, in proportion to the number of dwellings at each place, we get :

$$n_{virtual}(r) = m^+_{rent}(r).\max(1, \frac{D-S}{S_{rent}}) \tag{A.13}$$

and then :

$$n^*(r) = n(r) + \max(\mu(r), 0) + m^+_{rent}(r) \cdot \max(1, \frac{D-S}{S_{rent}}) \tag{A.14}$$

$n^*(r)$ can be different from the actual number of dwellings $\frac{H(r)}{q(r)}$. Anticipating that rents have an impact on dwelling size $q(r)$, but taking $n^*(r)$ and $H(r)$ as given, we can compute the rent $R^*(r)$ which adjusts dwelling size so that the number of dwellings becomes equal to $n^*(r)$:

$$R^*(r) = \beta \frac{(Y - T(r))}{H(r)} n^*(r) \tag{A.15}$$

If a location is attractive, and more people want to live there, $R^*(r)$ will be bigger than $R(r)$. On the contrary, if some dwellings are empty, $R^*(r)$ will be lower than $R(r)$. We suppose that landowners vary their rents to set them equal to $R^*(r)$, with the timescale τ_R:

$$\frac{dR(r)}{dt} = \frac{R^*(r) - R(r)}{\tau_R} = \frac{1}{\tau_R}\left(\beta \frac{(Y - T(r))}{H(r)} n^*(r) - R(r)\right) \tag{A.16}$$

Appendix A.5. Housing production function

Buildings depreciate, and are renewed or rebuilt by land owners in reaction to rental profitability. We suppose that some of them have a myopic behavior: they make investment decisions as if they were at a stationary state of equilibrium, and that some others make anticipations, and compares rents to rents that households would pay in an equilibrium state where all locations would have the same utility $\bar{u}$.

Housing $H'(r)$ is produced using land $L'(r)$ and capital $K'(r)$. The housing production function reads, in a classic way ([34, 60]):

$$H'(r) = AL'(r)^a K'(r)^b \tag{A.17}$$

where A, a and b are coefficients ($a+b=1$), $H'(r)$ the housing surface built, $L'(r)$ the ground surface occupied by the buildings and $K'(r)$ the financial capital used for construction. The benefit of land owners reads therefore:

$$\Pi(r) = (R(r) - R_0)H(r)' - \delta K(r)' \tag{A.18}$$

$\Pi(r)$ is the profit, δ represents the joined effect of real estate capital depreciation, annual taxes payed by landowners on the real estate capital, and interest rate. Developers build to maximize their profit: at each point of the metropolitan area they construct, i.e. choose $K'(r)$, to maximize $\Pi(r)$ under the constraint that $\frac{H'(r)}{L'(r)}$ ratio is limited by an urbanism constraint (see detail in Section 3.1). The metropolitan area boundary is defined by a rent R_0, below which it is not profitable to build housing building (this value corresponds both to other use of the land like agriculture and to the transaction cost in the building and renting process).

As for the other equations that we have presented, let us reason per unit of land: because $a+b=1$, we get

$$\frac{H'(r)}{L'(r)} = A\left(\frac{K'(r)}{L'(r)}\right)^b \tag{A.19}$$

So if we define $H(r) = H'(r)/L'(r)$ and $K(r) = K'(r)/L'(r)$, we have :

$$H(r) = A(K(r))^b \tag{A.20}$$

Developers seek to maximize their profits. Some of them have a myopic behavior: they make investment decisions as if they were at a stationary state of equilibrium. This leads to the optimal capital :

$$K^*_{myopic}(r) = \arg\max_{K(r)}(H(r)R(r) - \delta K(r)) \tag{A.21}$$

$$= \arg\max_{K(r)}(A(K(r))^b R(r) - \delta K(r)) \tag{A.22}$$

Some city landowners make anticipations, and compares current rents to rents that households would pay in an equilibrium state where all would have the same utility $\bar{u}$:

$$R_{anticipate}(r) = \alpha^\alpha \beta^\beta \left(\frac{Y - T(r)}{\bar{u}}\right)^{\frac{1}{\beta}} \tag{A.23}$$

This leads to the optimal capital:

$$K^*_{anticipate}(r) = \arg\max_{K(r)}(A(K(r))^b R_{anticipate}(r) - \delta K(r)) \tag{A.24}$$

We suppose that half of the the land owners are myopic, and half make anticipations, which leads to an amount of capital:

$$K^*(r) = \frac{K^*_{myopic}(r) + K^*_{anticipate}(r)}{2} \tag{A.25}$$

Let us define $H^*(r) = A \cdot K^*(r)^b$ the corresponding optimal housing quantity.

Construction and building depreciation take time. We suppose that financial investments are transformed into buildings with a time lag τ_H, which corresponds to the time required to achieve the construction. We also suppose that a decrease in $H(r)$ can happen through depreciation only, with the timescale τ_{dH}. Housing quantity dynamics is therefore given by :

$$\frac{dH(r)}{dt} = \begin{cases} \frac{H^*(r)-H(r)}{\tau_H} = \frac{AK^*(r)^b-H(r)}{\tau_H} & \text{if } H^*(r) \geq H(r) \\ -\frac{H(r)}{\tau_{dH}} & \text{if } H^*(r) < H(r) \end{cases} \tag{A.26}$$

Appendix B. Data and coefficients

Table B.1 and B.2 present the numerical data we used in our simulations. In absence of adequate data for some parameters, for instance the cost of time and construction costs, some parameters have been calibrated on the Paris structure in 2008 ([29]). These calibrated parameters are listed in tab. B.2.

The calibration of parameters τ_H, τ_n, τ_R and τ_q is particularly difficult. In this analysis, we assume that the timescale of population density and rents evolution is 3 year, whereas for dwelling size evolution it is 20 years. We also assume that building construction takes approximately 2 years. We have therefore chosen $\tau_R = \tau_n = 3$ years, $\tau_q = 20$ years and $\tau_H = 2$ years.

Similarly, it is difficult to assess the depreciation rate τ_{dH} of Paris buildings. We use here a depreciation timescale of 100 years (consistent with Wilhelmsson [61], for instance).

Considering the uncertainty in these parameters, we carried out a sensitivity analysis, varying each parameter independently, or simultaneously. We found that the qualitative results and order of magnitude presented in this paper are unchanged within a broad range of values (e.g., from 1 month to 20 years for τ_H, τ_n and τ_R, from 1 month to 100 years for τ_q , and from 50 to 200 years for τ_{dH}).

Appendix B.1. Maximum floor-area ratio in the center of Paris

Data lead to 1.5 as the value of the maximum floor-area ratio in the center of Paris. This value may seem low as most buildings in Paris have approximately 6 floors, which would induce a ratio of about 6 at the center of Paris. However, our ratio is only taking into account housing surface, and not the total built surface, and the discrepancy is simply caused by built surface intended for purposes other than housing (it includes, on the one hand, corridors and lobbies in buildings dedicated to housing and, on the other hand, all buildings not dedicated to housing: offices, shops, museums, train stations, office buildings, schools, universities, etc.).

Appendix B.2. Construction costs in 2008

The calibration process provides construction costs between 1173€/m^2 for a floor-area ratio of 2 and 794€/m^2 for a ratio of 1. We compare in Fig. B.1 the calibrated costs to construction cost estimates from the Centre Scientifique et Technique du Bâtiment (CSTB), a French public

Main Data	
Urban area population	French census figures for Paris urban area until 2008 and demographic scenario for 2009-2100 (Section 4.2).
Households average income	Households disposable income (Source: INSEE and J. Friggit) until 2008 and techno-economic scenario for 2009-2100 (Section 4.1).
Fraction of ground surface devoted to housing	Source: Corine Land Cover. In places where building is possible, the maximum fraction of ground surface devoted to housing is 62%
Maximum floor-area ratio in the center of Paris	1.5 (Appendix B.1)
Transport times in Paris urban area	Data used in [62]
Public and private transport prices	Data used in [48] until 2008 and techno-economic scenario for 2009-2100 (Section 4.1). We only deal here with perceived travel cost, and not with real travel cost which would also include vehicle amortization.
Interest rate	$\delta = 5\%$
Built capital depreciation time	$\tau_{dH} = 100$ years
Dwelling size evolution time constant	$\tau_q = 20$ years
Rent evolution time constant	$\tau_R = 3$ years
Population density evolution time constant	$\tau_n = 3$ years
Housing stock evolution time constant	$\tau_H = 2$ years

Table B.1: Summary of main input data

Calibrated parameters	
Households utility function parameter (Appendix A)	$\alpha = 0.7$
Coefficients of construction cost function (Appendix A)	$A = 2.0140$ and $a = 0.36$ in 2008 (Appendix B.2). Coefficient A evolves proportionally to $(income)^{-(1-a)}$
Cost associated with travel time	cf. Appendix B.3
Rent determining city border	$R_0 = 12€/m^2$ in 2008, and evolution proportional to income.
Logit factor used to compare different transport modes at each location	$factor = 4$

Table B.2: Summary of calibration parameters

institution providing analysis and research on construction and housing issues. These data are partial, since they are prices announced by developers in several public procurement documents and in various estimates of building construction costs, as well as technical documents. What emerges from CSTB data is an average cost of construction of 1200 €/m^2 before tax, or approximately 1400 €/m^2 including all taxes, which increases slightly as the building becomes higher. However, these estimates are quite uncertain: because of the diversity of types of buildings that it is possible to build, it is difficult to obtain a cost that can be used as a reference cost. The order of magnitude of the calibrated cost seems to agree with the order of magnitude of the data. These data present however a less convex profile than calibrated data. An explanation of the discrepancy may be that the so-called “actual" costs in CSTB data are direct construction costs, while in reality developers consider also additional costs when the height of buildings increases ([63]). These additional costs include administrative costs (building permits etc.), financial costs (the risk associated with a larger investment cost), and technical costs (duration and technical difficulty of the works), which may introduce more convexity in the real cost curve.

Appendix B.3. Cost of time in 2008

In the model, rents (per surface unit) decrease when moving away from the center of Paris because households have to pay a generalized transportation cost, which is the sum of a perceived monetary cost (interpreted here as the cost of fuel) and of the cost associated with transport time, assuming that households do a round-trip per day towards the center of Paris. In the simulation, cost associated with transport time represents generally the bigger part of generalized cost, and the way we assess this cost has an important role in our results.

Numerous studies have dealt with this issue, but no conclusive result exists on this complex subject. In Ile-de-France, French Government’s Strategic Analysis Center proposed to use net hourly wage as an estimate for commuting time cost, but explained that the value of actual

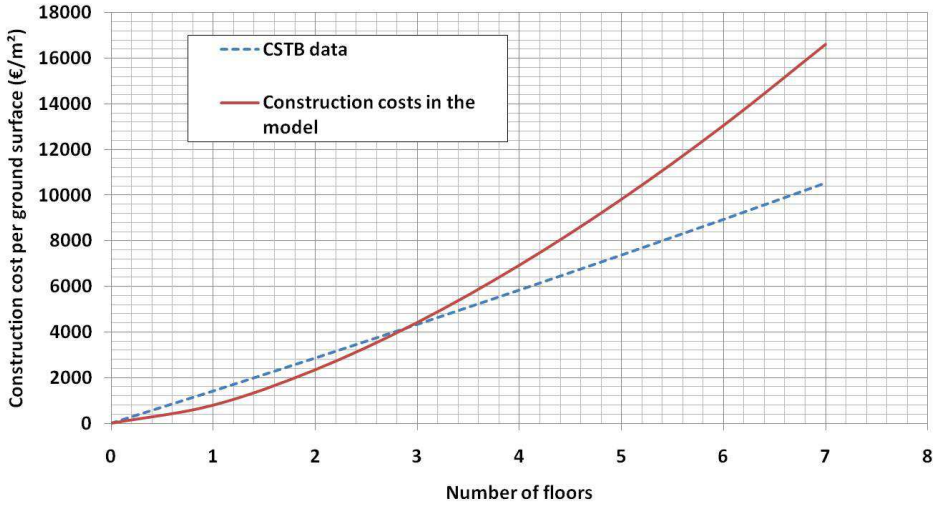


Figure B.1: Construction costs

commuting time cost depends greatly on several factors such as households characteristics or modal choice ([64]).

Due to the importance of time cost choice in the simulation, we calibrated time cost instead of using an a priori fixed value. We computed this cost using our data on rent spatial distribution: out of these data, assuming our model perfectly exact, it is indeed possible to estimate a theoretical generalized transportation cost. Assuming that this generalized cost reflects the sum of the direct cost of transport and of the cost associated with transport time, and assuming that households do a round-trip per day towards the center of Paris, the transport time cost was estimated as a function of journey time.

Marginal time cost seems to decrease with travel time, and we chose to model simply this decrease using a piecewise affine function. This representation leads us to use a cost time worth 105% of the net hourly wage when the travel time is less than 25 min (or, equivalently, when the distance to the center of Paris is less than 15 km), then a very low cost (6.6% of the net hourly wage) for portions of journey in excess of this limit. The value of time for journeys during less than 25 min is therefore very close to commuting time cost in Ile de France according to French Government's Strategic Analysis Center.

This observed decrease in marginal time cost can be attributed to the limits of our approach, in particular to the monocentric framework and to the hypothesis that households do a round-trip per day towards the center of Paris. In the real world, in places where travel time exceeds 25 minutes, a large fraction of households do not commute to the center of Paris. This leads to a shorter average trip length than in the mono-centric case, and using actual average trip length would enable to use more realistic time cost values and smaller total fuel costs for locations far from Paris city center. In absence of needed data, we did not take into account explicitly this variation in trip length, and modeled it with a non-linear time cost.

Appendix C. Link between Imaclim-R outputs and NEDUM-2D inputs

Local and global variables. In this study, four quantified evolutions are driving NEDUM model simulations: households average income evolution, city total population evolution, public transport price evolution, and private transport price evolution (cf. Sec. 4).

These variables describe evolutions taking place in Paris urban area, and are therefore *local*. An important question which arises when downscaling global scenarios is when should these local driving variables be consistent with global evolutions, i.e. when should local evolutions be determined by global evolutions, or when is it more interesting to consider that they are independent.

Here, we suppose that income, and transport prices evolutions are driven by global evolutions, whereas urban area total population is independent. As Imaclim-R is disaggregated into 12 regions, one of them being EU-27 and Turkey as a unique region, this means that we only consider scenarios in which Paris will inevitably follow locally decarbonisation and vehicle electrification trends determined by the model for this entire "Europe + Turkey" region. Conversely, world population growth in Imaclim-R are disconnected from Paris assumption from INSEE and the UN.[20]

What should be determined by local scenarios, or what should be independent, depends on the questions which one wants to address. Our choice was motivated by the fact that we did not aim here to analyze local policies influencing private vehicle technology choice in Paris (such as, for instance, local taxes dependent on households vehicle technology). We also did not consider specifically how local land-use policies could impact income levels. However, designing and assessing new local transport price or income scenarios disconnected from global scenarios would enable to study theses issues, and would be an interesting development from our work.

Imaclim-R / NEDUM-2D linkage. Imaclim-R provides many outputs, including for instance oil prices (cf. Fig. 5), but only three are used here in NEDUM-2D simulations : private vehicle usage cost per km, public transport usage cost per km and household income.

As Imaclim-R simulates averages over the entire Europe, we do not directly use Imaclim-R outputs in NEDUM-2D simulations. We suppose that, from 2009 on, NEDUM-2D input data evolve proportionally to Imaclim-R outputs. Input values until 2008 are therefore historical values, whereas values after 2009 are historical value in 2008, multiplied by the ratio between Imaclim-R value in that year over Imaclim-R value in 2008.

Table C.1 shows examples of the range of transport prices, households income and total population values used in NEDUM-2D simulations for two timesteps.

[20] Rigoroursly speaking, world population growth in Imaclim-R is driven by demographic scenarios inspired by the UN, but, depending on the simulation, demographic scenario choice in Imaclim-R can be the same or can be different from UN scenario choice underlying demographic scenario in Paris urban area.

	2050				2100			
	SN	LN	SY	LY	SN	LN	SY	LY
Average cost to drive 1km in private vehicle, including electric vehicles and carbon tax (€/km)*	8.1	9.7	8.2	10	6.9	6.4	5.2	6.6
Monthly cost of basic public transport pass (or equivalent), including carbon tax (€/month)*	50	73	48	74	52	52	38	45
Average annual household disposable income (k€/year)*	129	133	129	132	315	221	272	220
	Low scenario		High scenario		Low scenario		High scenario	
Population**	6 370 000		6 370 000		5 610 000		6 370 000	

* See Fig. 6 for other years.
** See Fig. 7 for other years.

Table C.1: NEDUM-2D model input data for years 2050 and 2100. Average cost to drive, monthly cost of public transport pass and annual household disposable income are computed based on Imaclim-R corresponding outputs. Population evolution scenarios are independent from Imaclim-R outputs and parameters. Data for each year between 2008 and 2100 are plotted in Fig. 6 and 7.

Appendix D. The IMACLIM-R parameters

The Imaclim-R global scenarios are part of the 576 scenarios designed for Rozenberg et al. [47].

			Assumption 1 (LN and LY scenarios)	Assumption 2 (SN and SY scenarios)
Oil and gas markets	**Oil**	**Amount of ultimately recoverable resources (total conventional and non conventional)**[***]	3.6 Tb	3.1Tb
		Inertia in the deployment of non conventionals (spread of the bell-shaped curve for each field)	no inertia (b=0.061)	inertia (b=0.041)
		Maximum growth rate of Middle-East capacities	0.8Mbd/year	0.7Mbd/year
		Remaining resources before depletion starts	25%	50%
	Gas	Indexation of gas price on oil price	Until 80$/bl	Always indexed
OPEC behavior		Target oil price	40$/bl	80$/bl
Coal		Price growth elasticity to production decrease	1.5	1
		Price growth elasticity to production increase	1	4
		Production growth rate which cancels out price growth rate	2%	0,05%
Power generation decarbonization	**Nuclear**	**Maximum market shares [min - max]**[**]	[2.5% - 20%]	[5% - 40%]
	Renewables	Maximum market share of renewables	15%	25%
		Learning rate for renewables investment costs	3%	7%
	Carbon capture and storage	CCS learning rate	7%	13%
		CCS start date	2015	2010
		CCS "bottleneck phase"	10 years	7 years
		CCS maximum market share at the end of the bottleneck phase	3.5%	5%
		CCS growth phase	8 years	8 years
		CCS maximum market share at the end of the growth phase	63%	90%
		CCS maturation phase	8 years	8 years
		CCS maximum market share at the end of the maturation phase	70%	100%
Low carbon end-use technologies	**Electric vehicles**	EV start	No significant market penetration	
		EV "bottleneck phase"		3 years
		EV maximum market share at the end of the phase		2.5%
		EV growth phase		15 years
		EV maximum market share at the end of the phase		45%
		EV maturation phase		16 years
		EV maximum market share		50%
	Industry	Capital lifetime in the industry	30 years	20 years
	Energy efficiency	Freight energy consumption	1	Trend extracted from POLES data: starts at 1 reaches 1.1 in 2030 and stays at 1.1 until 2100
		Freight fuel consumption elasticity to fuel prices	-0.35	-0.4
		Buildings energy consumption per m^2[*]	Trend which starts at 1, reaches 1.2 in 2030 and stays at 1.2 until 2100	1

The parameters in bold are multiple parameters.
[*] different parameters according to the region.
[**] different parameters according to the region and horizontal slice in the annual monotonous load curve (between base load and peak load).
[***] different parameters according to the region and category of oil.

Table D.1: Parameters of the Imaclim-R global scenarios (see Rozenberg et al. [47]).

			Assumption 1 (LN and LY scenarios)	Assumption 2 (SN and SY scenarios)
Alternative liquid fuel supply	**Biofuels**	Time scale of reactive anticipation for biofuels production Biofuels supply: multiplier coefficient of the supply curves for the default value)	6 years Value from IEA curves	4 years 50% increase w.r.t Assumption 1 value
	Coal-to-liquids	Oil price threshold for CTL production start Time scale of reactive anticipation for CTL production Maximum production growth in 2030, 2035 and in 2050	200 $/bl 8 years 0.05 Mbd - 0.10 Mbd - 0.10 Mbd	120 $/bl 0 0.20 Mbd - 1.5 Mbd - 3 Mbd
Development patterns	**Transport**	**Motorization rate growth with GDP per capita***	50% increase w.r.t Assumption 2 value	Value from IEA data
	Buildings	Income elasticity of buildings stock growth Asymptote to surface per capita in China and India Start year and fuel price for a forced decline of oil consumption in this sector	1 60 2020 - 1300$/tep	0.7 40 2010 - 1000$/tep
	Industrial goods	**households industrial goods consumption saturation level [min-max]*** (multiplier factor of the calibration year consumption volume)	[1.5-3]	[1-2]

The parameters in bold are multiple parameters.
* different parameters according to the region.

Table D.2: (End of tab. D.1) Parameters of the Imaclim-R global scenarios (see Rozenberg et al. [47]).